Available online at www.sciencedirect.com
SCIENCE DIRECT®
Journal of Sound and Vibration 281 (2005) 21–44
JOURNAL OF SOUND AND VIBRATION
www.elsevier.com/locate/jsvi

Beat characteristics and beat maps of the King Seong-deok Divine Bell

Seock-Hyun Kim[a], Chi-Wook Lee[b,*], Jang-Moo Lee[c]

[a]*Division of Mechanical and Mechatronic Engineering, Kangwon National University, Choon-cheon, Kangwon-do, Korea*
[b]*Mechanical Engineering Department, School of Engineering and Computer Science, University of the Pacific, Stockton, CA 95211, USA*
[c]*School of Mechanical and Aerospace Engineering, Seoul National University, Sinlim-dong, Kwanak-gu, Seoul, Korea*

Received 9 June 2003; accepted 6 January 2004
Available online 15 September 2004

Abstract

King Seong-deok Divine Bell is the second oldest bell in Korea. The bell is considered to have the best sound quality among Korean bells. The beat phenomenon is one of the most important characteristics for the sound of the King Seong-deok Divine Bell. In this study, the relationships between the modal parameters and the peculiar beat phenomena of the bell are investigated. It is theoretically proved from the beat characteristics that the sound might indeed be heard differently depending on the listening positions. The beat map method is introduced to visualize the beat distribution properties. It is shown that the beat maps can be drawn with a theoretical model based on the modal data of the bell. Using the beat maps of the King Seong-deok Divine Bell, it is investigated why clear and unclear beats, large and small amplitudes of the vibrations are repeated periodically along the circumference of the bell. Furthermore, the effect of the striking position on the beat distribution property is examined systematically.

1. Introduction

Any nation can be proud of historic bells with good sound qualities and beautiful appearances since they reflect workmanship in its culture. In Korean history, manufacturing a large bell was

*Corresponding author. Tel.: +1-209-946-2151; fax: +1-209-946-3102
E-mail addresses: seock@kangwon.ac.kr (S.-H. Kim), clee@uop.edu (C.-W. Lee), leejm@gong.snu.ac.kr (J.-M. Lee).

0022-460X/$ - see front matter © 2004 Elsevier Ltd. All rights reserved.
doi:10.1016/j.jsv.2004.01.038

often a nationwide project in which many specialists including casting engineers, scientists, and artists were required to participate. Some of historic Korean bells exceed 10 000 kg and were manufactured several hundred, or even more than 1000 years ago [1]. A lot of people meditate and achieve spiritual enlightenment while listening to the magnificent and deep striking sound of a bell. In the western bells, the harmonic property of the frequency components is the most important factor for the pitch and timbre of the striking sound. Design and manufacturing methods have been studied in order to make bells with good sound qualities. Rossing [2,3] has investigated the various kinds of eastern and western bells to determine the relationships between their natural frequencies from the musical point of view. Perrin and Charnley have reported natural frequencies and mode data on a number of English church bells [4,5]. They introduced the tuning method to improve the sound quality of various bells [6]. However, there seems to exist somewhat of a difference between the East and the West in determining the quality of the bell sound. Although it is somewhat subjective, in Korean bells, three representative acoustic features are required for good sound. They are the magnificent and clean striking sound, the intermediate sound by the hum and the fundamental with a strong beat of the proper period, and the long-lasting hum with a clear beat [1]. The King Seong-deok Divine Bell is considered to have all of these features. Lee [7] has proposed a quantitative rating method for the striking sound of Korean bells. As a result, the King Seong-deok Divine Bell was estimated as the bell having the best sound quality among Korean bells. All Korean bells including the King Seong-deok Divine Bell have a beat that is a periodic repetition of the strong and the weak sounds. It results from the inevitable asymmetric distribution of mass and stiffness in the casting process and the asymmetric configuration with various carved figures on the bell surface [8–10]. Since a strong beat of a western bell is usually considered an undesirable property, called warble, bell makers in the West would try to remove it within reasonable limits [11]. For Korean bells, however, intervals between strikings are pretty long and people can get different feelings from the long-lasting beat of the hum, the fundamental, as well as the striking sound. A clear beat of the hum with a certain period makes people feel as if it were alive and breathing and the strong beat of the fundamental makes the bell as if it wails or cries [12].

The King Seong-deok Divine Bell is a huge structure over 3 m in height and larger than 2 m in diameter. The amplitude and the phase of each tone of the bell are different from one position to another position. As a result, audiences can hear quite different beating sounds depending on where they stand around the bell. With this background, the beat phenomenon has been an interesting research topic in Korean bells. On the beat phenomenon, Perrin et al. [11,13] have reported on the control of the warble characteristics of the western bells. Kim and Soedel [14] have analyzed the beat characteristics of a slightly asymmetric cylindrical shell as a bell-type structure. Lee and Kim [15] have proposed an experimental method to control the period and the clarity of beat on a large-scale Korean bell. They successfully produced a good beat in the hum by grinding out materials from the inside of the bell at proper positions. Recently, an interesting beat property has been detected during examination of the King Seong-deok Divine Bell [16]. By a series of experiments, it was confirmed that the clear and the unclear beats in vibration are repeated periodically on the circumference of the bell body. As a result of the beat in the vibration of the bell body, beating sound also radiates with directivity. In this paper, the beating properties of the King Seong-deok Divine Bell are examined in detail. It is investigated how the beats in vibration and sound are generated differently depending upon the positions on the bell surface. A drawing

method for a beat map using a mathematical model is introduced as a mean of visualization of the beat distribution property. Using the beat maps, the positions to feel the breathing of the long-lasting hum, or positions to hear the clear beat in the fundamental, are identified. The final goal of the study is to visualize the beat distribution property so that people can grasp at a glance where clear and unclear beats are generated.

2. The King Seong-deok Divine Bell

The King Seong-deok Divine Bell is well known by another nickname, '*Emillie Bell*.' '*Emillie*' means a crying sound of a child. In Korea, the famous tale of '*Emillie*' has been passed on from one generation to another. The bell was cast in A.D. 771 in the unified Silla Dynasty and its weight is 18.9 tons by recent measurement [12]. It is considered to be one of the Korean masterpieces with a historical casting background, a huge size, an artistic excellence, and the most of all, its magnificent and beautiful sound. As the 29th national treasure in Korea, this bell is now in Kyungjoo National Museum, Korea. Regular striking demonstrations have been stopped since 1991 for the conservation of the bell. However, with people's desire to hear the sound of this bell again, there was a comprehensive structural diagnosis including a test striking from 1996 to 1998 [12] and striking demonstrations have been carefully done once a year since 2001. Fig. 1 shows the picture of the bell along with the notations of the dimensions. The dimensions of major parts are listed in Table 1. The bell is a barrel-type axisymmetric shell as the basic structure and various

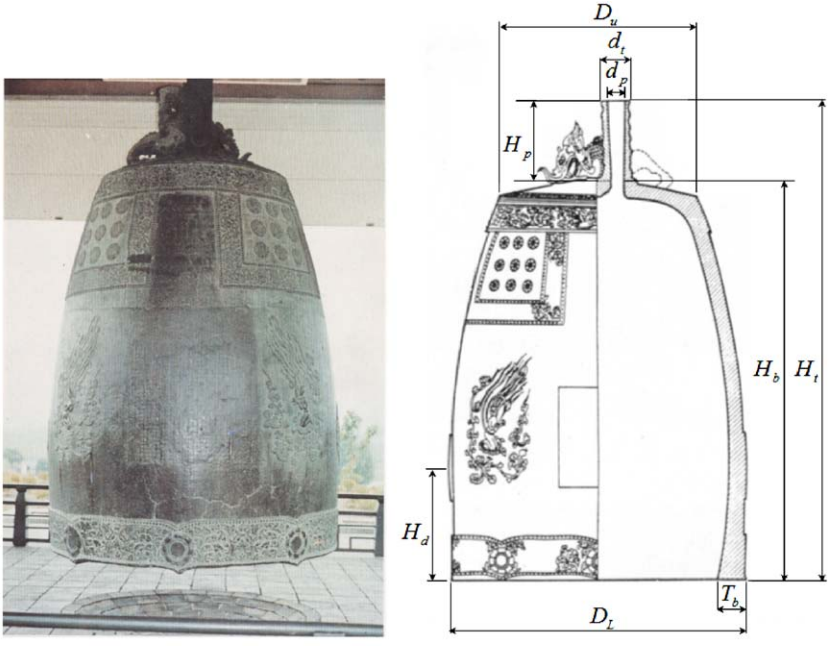

Fig. 1. The King Seong-deok Divine Bell: (a) picture of the bell, (b) notations for the dimensions.

Table 1
Dimensions of the King Seong-deok Bell

Parts	D_u	d_t	d_p	H_p	H_b	H_t	H_d	T_b	D_L
Dimensions (mm)	1510	230	48	633	3030	3663	856	203	2227

figures are carved on the surface. The top of the bell is shaped with a dragon-type sculpture. People admire the fact that it has endured its heavy weight and the dynamic load by innumerable strikings for more than 1200 years.

This large Korean bell is struck by a big wooden hammer, which is called *Dangmok*, while metal clappers are used for western bells. The striking method with the *Dangmok* may be advantageous to produce a low-frequency magnificent and deep sound instead of a sharp metallic sound. This bell has some interesting acoustic features: a sound pipe at the top of the bell, and a sound hollow below the body. The roles of the sound pipe can both be an acoustic filter and a support for the load [17,18], while the sound hollow produces a resonance effect so that the bell keeps its vibration for a long period of time [19]. The striking position, called *Dangjwa*, is designed to minimize the reaction force at the hanging point by positioning it around the center of percussion of the entire structure. Recently, based upon the precisely measured data, Lee and Kim [20] have calculated the center of percussion (H_d in Fig. 1) as 625 mm.The ratio of the difference between the measured and the calculated centers of percussion on the total height is only about 6%. All the features mentioned above indicate that bell makers in the unified Silla Dynasty of 1200 years ago had a high level of bell manufacturing technology.

3. Vibration and sound properties of the King Seong-deok Divine Bell

3.1. Measurement of sound and vibration

Fig. 2 shows the experimental setup for measuring vibration and sound during a striking ceremony. A wooden hammer strikes the *Dangjwa* at the height of H_d, measured from the bottom of the bell (see Fig. 1(b)). Acceleration signals are acquired from the equally spaced 24 measurement points on the circumference and 4 points on different heights along the contour of the bell as shown in Fig. 3. The signals acquired from Point 2 in Fig. 3 were used as a reference to monitor the variations of the impact force. On the other hand, sound signals were measured at the distances of 20 cm and 2 m from the accelerometers as shown in Fig. 3.

3.2. Measurement results

Fig. 4 displays the power spectra of acceleration and sound signals at the instant of striking. More than 50 frequency components below 1000 Hz exist while there are more than 130 components below 2000 Hz to produce sound. Frequency components in sound are matched with those in vibration, i.e. the natural frequencies of the bell. The sound power of each frequency component is determined by striking conditions, measurement positions, the configurations of

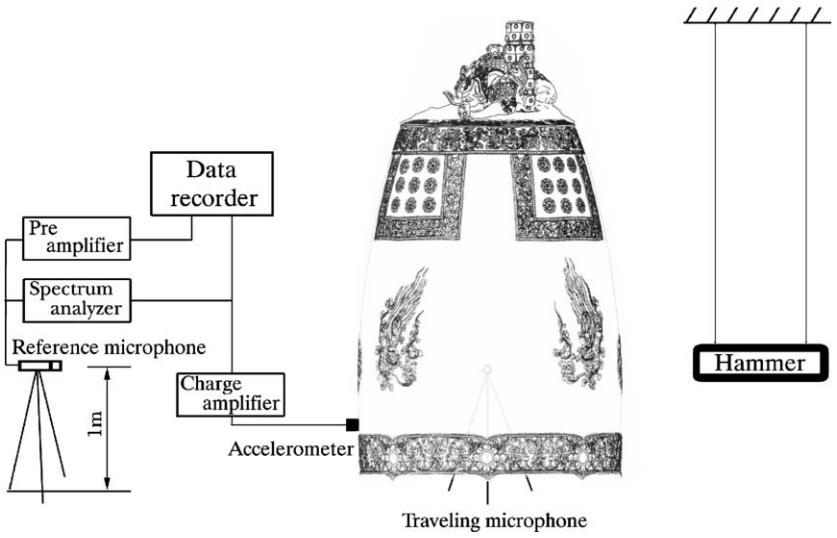

Fig. 2. Experimental setup for measuring vibration and sound.

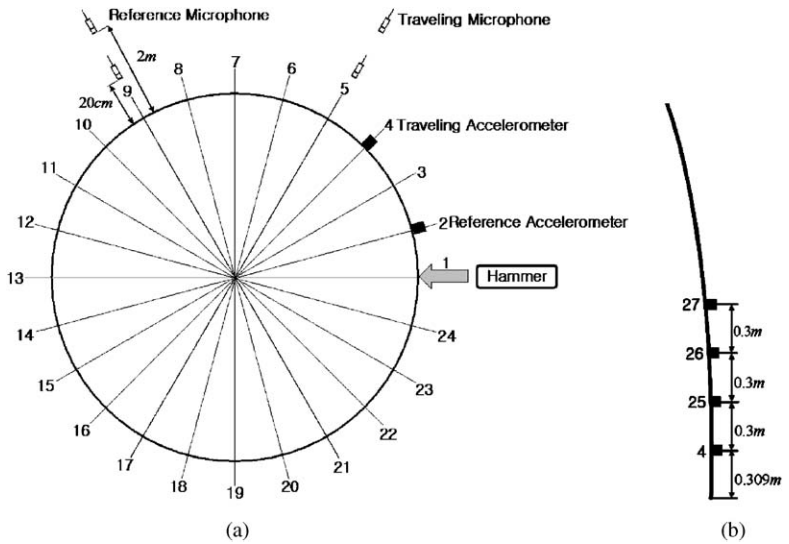

Fig. 3. Measurement positions: (a) top view, (b) side view.

each vibration mode, and the sound radiation properties, etc. Table 2 shows the frequency components of the lower partials. Modes are indicated by the symbol for the mode of a cylindrical shell. The *mode* (m, n) represents the vibration shape that has m nodal circles on the height and $2n$ nodes on the circumference. Each mode has a mode pair indicated by $(m, n)_L$ and $(m, n)_H$. For each mode pair, the subscript L indicates the mode with a slightly lower frequency, while the subscript H is used for the mode with a higher frequency. The modes are identified by a modal test that will be described in the next section.

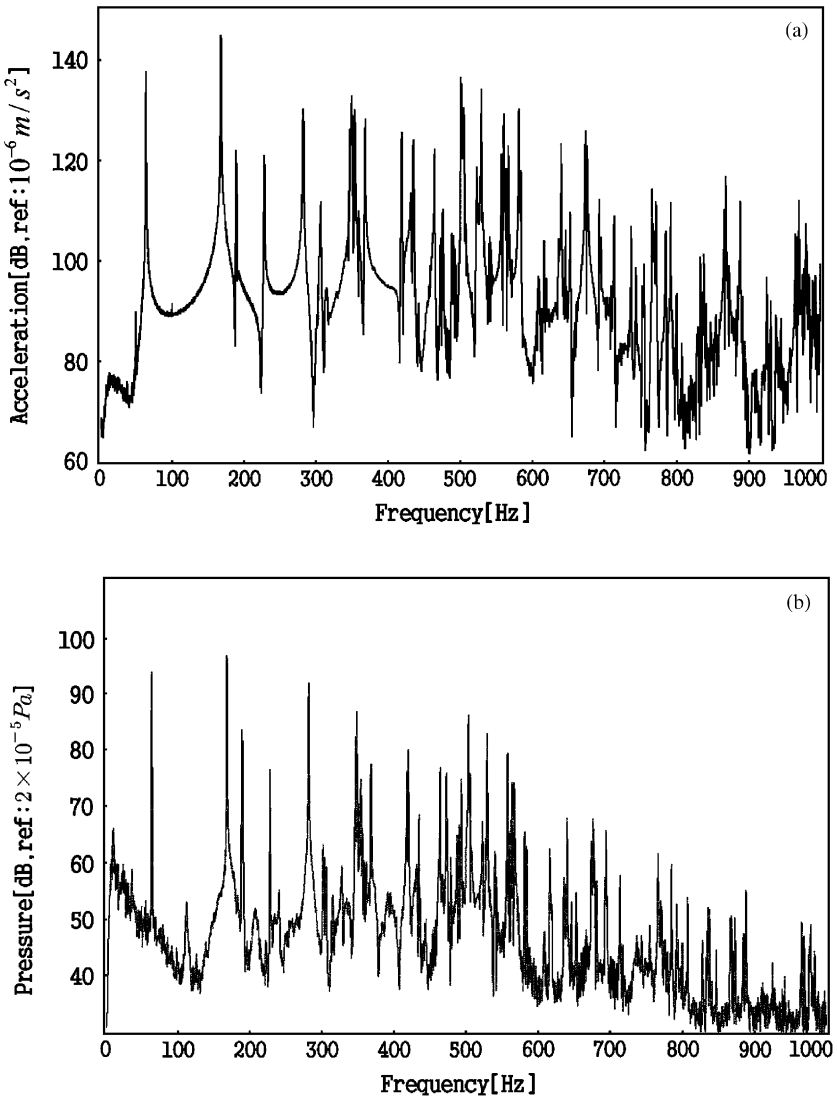

Fig. 4. Power spectra of the signal at the instant of the striking: (a) vibration (b) sound.

The tonality of the striking sound is determined by the harmonic relationships of the frequency components. The striking sound of the bell is contributed to largely by the lower partials of 64, 168, 190, 228, 282, and 350 Hz [7]. The *mode* (*0, 2*) and *mode* (*0, 3*) produce the hum and the fundamental, which are very important components in the aspect of the beating sound of the bell.

Fig. 5 shows how the frequency components in vibration and sound are decaying with time. All the partial tones except the hum and the fundamental disappear in several seconds and in 20 s after a strike the hum only remains. Therefore, after several seconds, the hum and the fundamental will dominate the sound of the bell. In the long lasting hum, the strong and the weak are repeated periodically every 3 s. This beat makes the low-frequency hum last long as if the bell

Table 2
Natural frequencies and modes of the King Seong-deok Divine Bell

No.	*Mode* (*m*, *n*)	Frequencies (Hz)	
		Measurement	FEM [20]
1	$(0, 2)_L$	64.07	64.10
	$(0, 2)_H$	64.42	64.30
2	$(0, 3)_L$	168.52	171.27
	$(0, 3)_H$	168.63	171.93
3	$(1, 2)_L$	189.34	206.22
	$(1, 2)_H$	190.55	209.05
4	$(1, 3)_L$	227.99	241.75
	$(1, 3)_H$	228.34	242.27
5	$(0, 4)_L$	281.93	295.23
	$(0, 4)_H$	282.61	297.87
6		347.27	
		348.79	
7	$(1, 4)_L$	349.40	358.20
	$(1, 4)_H$	350.12	366.53

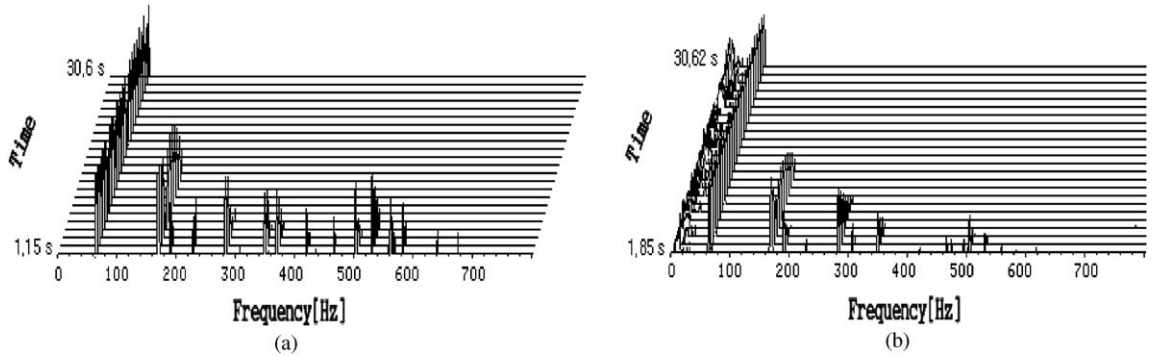

Fig. 5. Three-dimensional spectra of vibration and sound: (a) vibration, (b) sound.

is breathing. In the three-dimensional spectra, the fundamental with the frequency of 168 Hz shows a strong beat with a period of 9 s. It breaks off one time and then revives. The 168 Hz fundamental is responsible for the clarity of the sound and its strong beat gives the impression that the bell wails. Another interesting phenomenon is that the wave patterns or the spectra of the vibration and sound occur quite differently depending on the location on the circumference of the bell. This makes people hear different sounds depending on the hearing position. Consequently, the magnificent and beautiful striking sound created by the mixture of a number of partial tones, the clear and strong beat of the fundamental for about 20 s after striking, and the long-lasting breathing beat of the hum are the three important features in the sound of the King Seong-deok Divine Bell.

4. Vibration modes of the King Seong-deok Divine Bell

4.1. Measurement and analysis of vibration modes

As shown in Fig. 1, the King Seong-deok Divine Bell is a very massive structure and it is hung at the belfry. This makes it difficult to generate modes using a general commercialized impact hammer or exciter. The mode pair $(0, 2)_L$ and $(0, 2)_H$ generate the hum and its beat, while the mode pair $(0, 3)_L$ and $(0, 3)_H$ produce the fundamental and its beat. These mode pairs have very close frequencies as shown in Table 2. In this study, a loud speaker and a frequency generating system are used to resonate $(m, n)_L$ and $(m, n)_H$ mode pairs separately. For the effective resonance, the speaker was put at the anti-node position of each mode and the bell is accurately excited by each natural frequency without producing any beat. Comparing the 24-point signals with the reference signal at Point 2 makes it possible to determine the magnitude and the phase of the acceleration at each position in Fig. 3. The mode shapes are obtained by Eq. (1) for the Operational Deflection Shape (ODS_j) [21].

$$\mathrm{ODS}_j = \frac{S_{jR,i}}{S_{RR,i}}\sqrt{S_{RR,i}} = H_{jR}\sqrt{S_{RR,i}}\,, \tag{1}$$

where $S_{jR,i}$ is the cross-spectrum of jth point signal with respect to the reference signal at ith measurement. $S_{RR,i}$ is the auto-spectrum of the reference signal at ith measurement while H_{jR} represents the frequency response function of jth signal to the reference signal.

4.2. Mode shapes

In Fig. 6, the measured *modes* (*0, 2*) and (*0, 3*) are plotted on the circumference at the positions with 15° increments and along the contour of the bell. Each angular position is designated counterclockwise from the top view with the striking position as a reference point, i.e., zero degree. In Fig. 6(a), the pair of the *mode* (*0, 2*) has almost 45° phase difference on the circumference. Around the striking position, the node of the *mode* $(0, 2)_L$ is at the position of $-8°$ and the node of the *mode* $(0, 2)_H$ is located at 36°. Therefore, the present striking position excites the *mode* $(0, 2)_H$ strongly and this condition produces the clear beat with a small amplitude at particular positions. In Fig. 6(b), the node of the *mode* $(0, 3)_L$ is located at 16° while the node of the *mode* $(0, 3)_H$ is at $-15°$. Therefore, the striking position becomes the center of the two nodes and the pair of *mode* (*0, 3*) is equally excited. This configuration of the mode pair and striking position satisfies the condition for a strong beat in the fundamental. For a three-dimensional mode shape, authors have performed a finite element analysis on the King Seong-deok Divine Bell [20], using the experimentally measured data [12]. The results shown in Fig. 7 are very close to the measured modes even with the limited number of measuring points. Since the bell is a barrel-type symmetric shell as basic structure, the measured and calculated frequencies are matched very well in the low-frequency modes, as shown in Table 2. However, they show somewhat large discrepancies for the positions of nodes and anti-nodes on the circumference since it was practically impossible to accurately model a slightly asymmetric distribution of mass or stiffness. This means that the natural frequency and the mode are predictable to a certain degree in a design stage, but it is almost impossible to predict the beat properties of any bell.

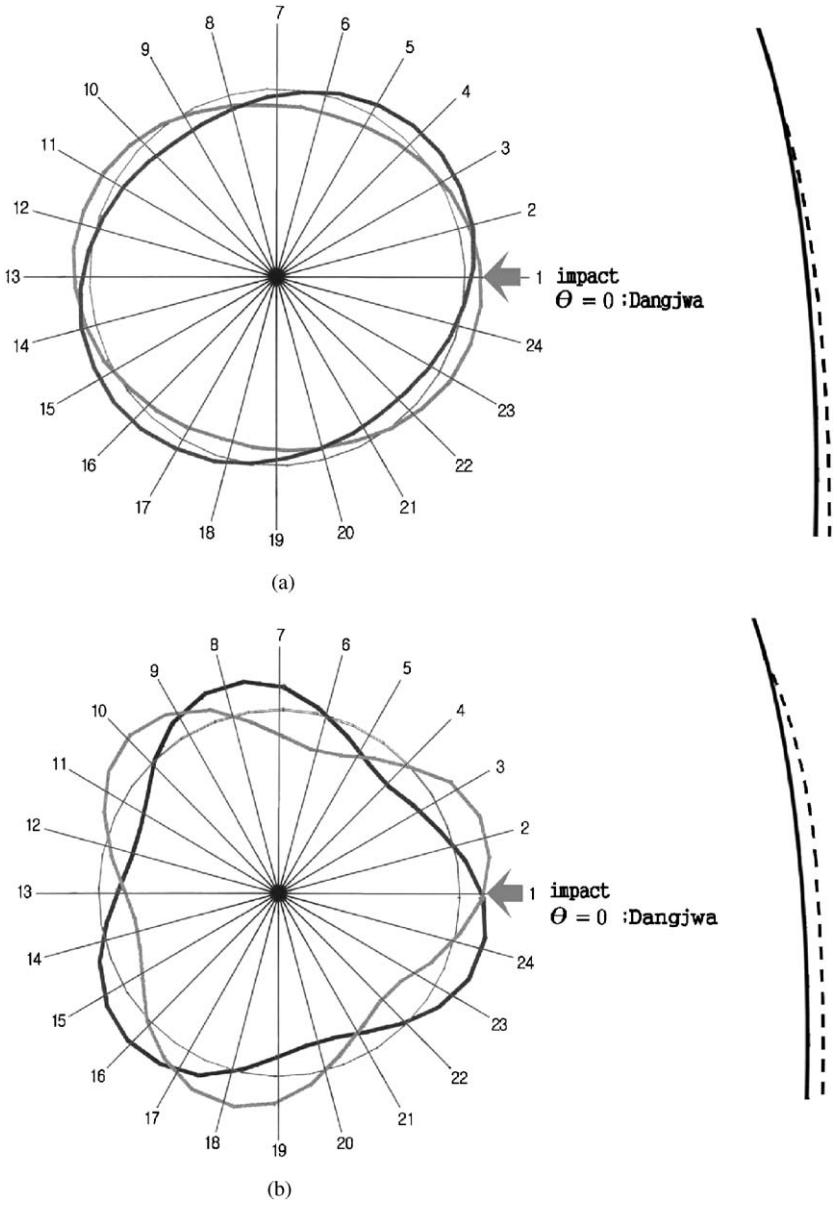

Fig. 6. Vibration mode pairs by measurement. (a) *Mode* (*0, 2*): —, *L-mode* 64.07 Hz; —, *H-mode* 67.42 Hz. (b) *Mode* (*0, 3*): —, *L-mode* 168.52 Hz; —, *H-mode* 168.63 Hz.

5. Experiments on the beat of the King Seong-deok Divine Bell

5.1. Wave distribution of the striking sound and vibration

Fig. 8 shows a distribution pattern of vibration waves at 24 different points of the circumference and 4 points at different heights along the contour. Signals are acquired for 20 s starting

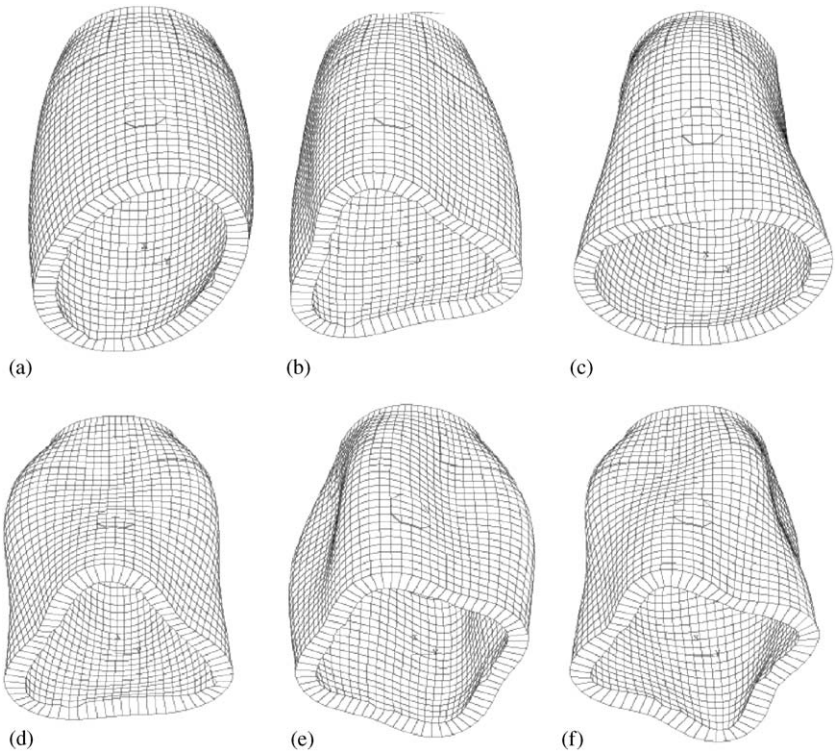

Fig. 7. Vibration modes of King Seong-deok Divine Bell by finite element analysis [20]: (a) *Mode* (*0, 2*), (b) *Mode* (*0, 3*), (c) *Mode* (*1, 2*), (d) *Mode* (*1, 3*), (e) *Mode* (*0, 4*), (f) *Mode* (*1, 4*).

from 3 s after the strike and they are plotted on each measuring point. At each striking, the swing angle and the speed of the hammer are uniformly maintained to keep the striking force constant. The variance of the striking forces is confirmed to be very small with the signals from the reference accelerometer installed at Position 2 in Fig. 3. In Fig. 8, the waves near the front striking position at Point 1 and at every 90° incremental position from it have large amplitude. However, the waves at these positions do not show clear beats. Rather, clear beats are produced inbetween the unclear beat positions. The decrease in magnitudes, while maintaining the wave patterns, is observed from the waves recorded at the four different heights along the contour. Sound measurements were possible only at 14 different points because of the limited experimental environment during the demonstration ceremony. Fig. 9 shows that the beating sound with the period of 3 s has an periodical distribution on the circumference following the vibration. As the distance from the bell increases, only the magnitude of wave decreases as predicted. As previously stated, higher partials except hum and fundamental disappear in several seconds. The long-lasting hum dominates the beating wave in the wave distribution charts. To understand the beat distribution characteristics in detail, the wave distribution chart of each tone (called the *beat map* hereafter) is investigated in the next section.

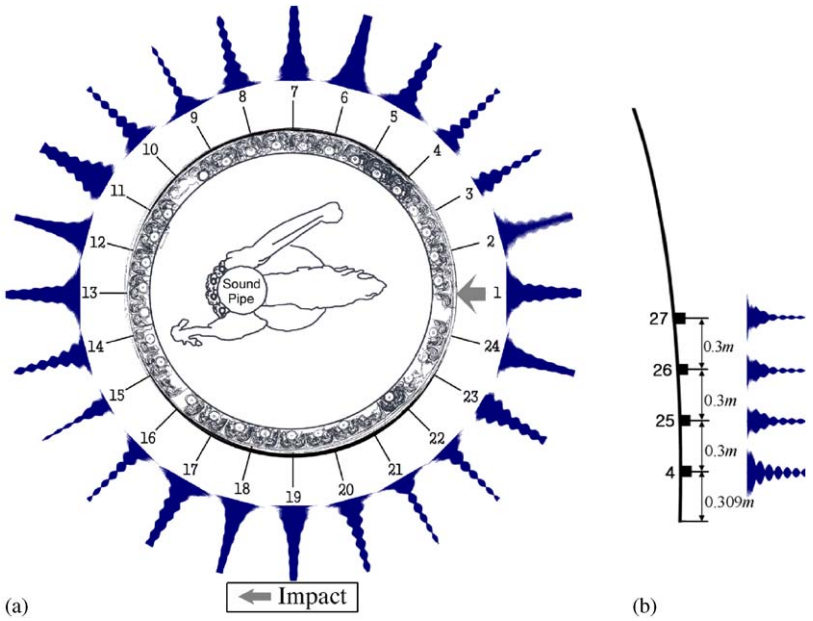

Fig. 8. Vibration wave distribution charts on the bell surface: (a) top view, (b) side view.

5.2. The beat map of the hum

In order to find the beat characteristics of the hum, only the frequency components of the *mode* (*0, 2*) pair are extracted with a bandpass filter. Fig. 10 compares the vibration signals at two different points under the normal striking conditions. A clear beat appears at Point 9, but not at Point 11. However, the magnitude of the wave at Point 11 is larger than that at Point 9. This result means that the power of the sound is different according to the position on the circumference of the bell. Also, one part produces a clear beat while another part produces an unclear beat. In Fig. 10(a), the period is calculated as 2.9 s and this value exactly corresponds to the inverse of the frequency difference, 0.35 Hz for the mode pair $(0,\ 2)_L$ and $(0,\ 2)_H$. Until the bell sound disappears completely, the beat of the vibration *mode* (*0, 2*) creates the impression that the low-frequency hum is breathing.

To understand the beat distribution properties of the hum, the beat map is introduced. Fig. 11 shows a beat map of the hum. After filtering the hum from the sound and vibration, the first 10-s waves are plotted radially at each measuring point on the circumference.

The beat map of the hum shows that vibrations with large amplitudes, without clear beats, are generated at the front striking position and at every 90° incremental position from it (Points 1, 6, 7, 12, 13, 18, 19, and 24). On the other hand, clear beats are generated inbetween those unclear beat positions (Points 3, 4, 9, 10, 15, 16, 21, and 22). This beat distribution pattern is similar to that of Fig. 8, as the hum strongly influences the entire wave, except the instant of striking. The beat map of the sound is almost identical to that of the vibration in periodic distribution characteristics. This occurs because the vibration velocity of the bell surface

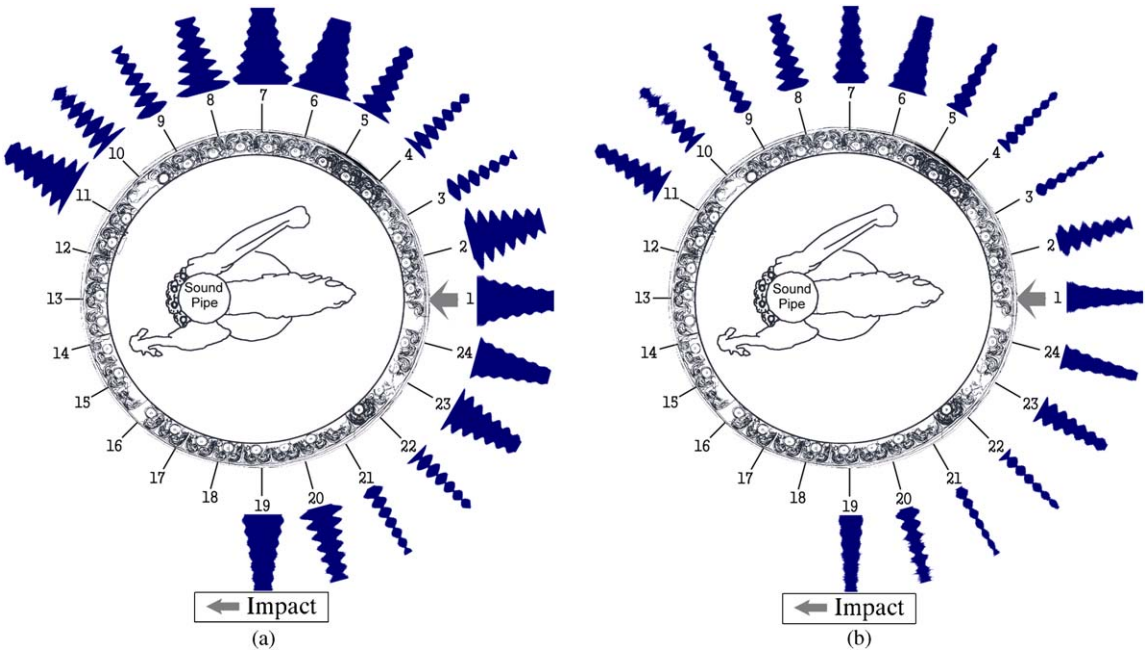

Fig. 9. Sound wave distribution charts on the bell surface: (a) 20 cm distance, (b) 2 m distance.

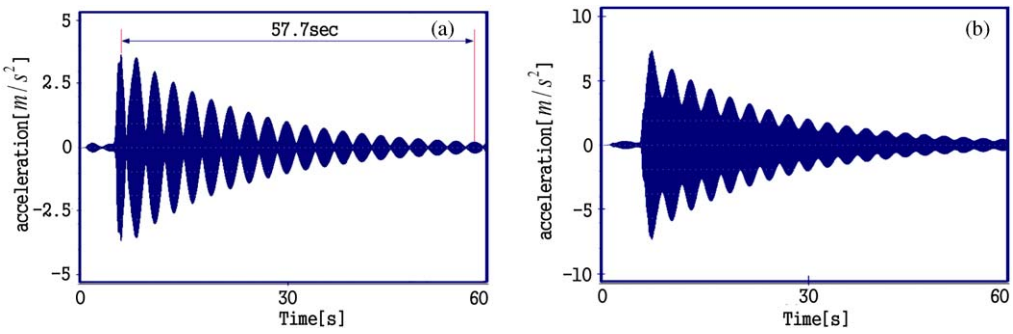

Fig. 10. Beat in the vibration of the hum (by 62–66 Hz digital filtering): (a) Point 9, (b) Point 11.

determines the sound pressure around the bell surface. Consequently, if audiences want to hear the breathing beat in the long lasting hum, they need to position themselves at Points 3, 4, 9, 10, 16, 21, or 22.

5.3. *Beat map of the fundamental*

Another important property observed in the measurement is the beating sound of the fundamental. The fundamental has a frequency of 168 Hz, which is more audible than the hum of 64 Hz. Audiences often say that for about 20 s after striking, the clear sound strongly occurs. It

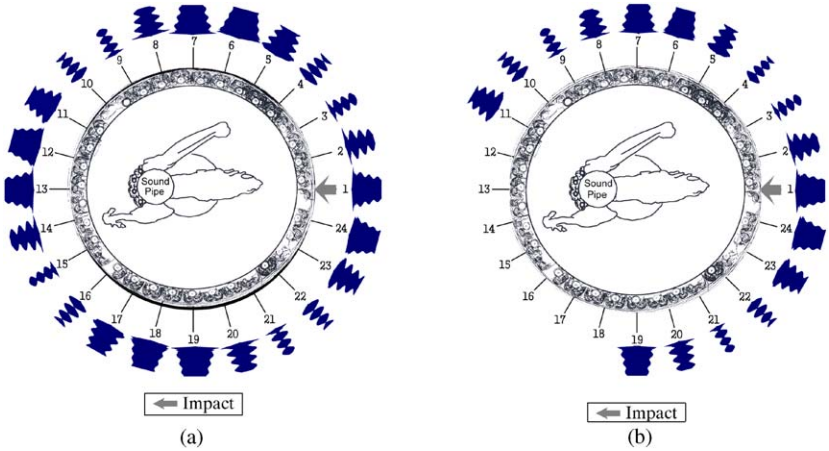

Fig. 11. Beat maps of the hum (*mode* (*0, 2*)): (a) vibration, (b) sound.

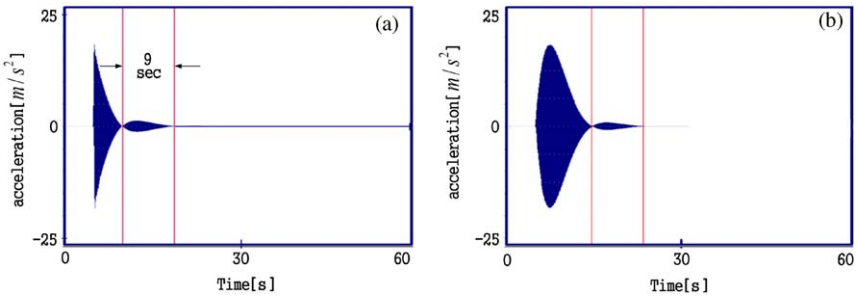

Fig. 12. Beat in vibration of the fundamental (by 165–175 Hz digital filtering): (a) Point 9, (b) Point 11.

disappears for a moment and then revives again. The bell seems to wail. This characteristic of the sound is confirmed by the filtered waves of the fundamental in Fig. 12.

In Fig. 12, the period of the fundamental is measured as 9 s. This value corresponds to the inverse of the frequency difference, 0.11 Hz of the two natural frequencies at 168.52 Hz and 168.63 Hz of the mode pair $(0, 3)_L$ and $(0, 3)_H$. The second one after the first strong vibration occurs weakly because of the large modal damping of the mode pair $(0, 3)_L$ and $(0, 3)_H$. As a result, the second weak sound could only be heard when the bell is strongly struck. An interesting phenomenon in Fig. 12 is that at Point 11, the sound energy gradually increases and then decays, while at Point 9, the maximum power occurs at the instant of striking and soon decays. It indicates that the times for the maximum and minimum powers in vibration are different from one position to another position. This makes people hear different resultant sounds depending on listening positions. The beat of the fundamental also periodically distributes on the circumference because of the periodic nature of the mode pair. Fig. 13 shows the beat map of the fundamental, drawn from the 20-s filtered waves.

A clear beat is observed at every 30° incremental position such as Points 1, 3, 5, etc., from the striking position. However, there is no beat at even number of positions such as Points 2, 4, 6, and

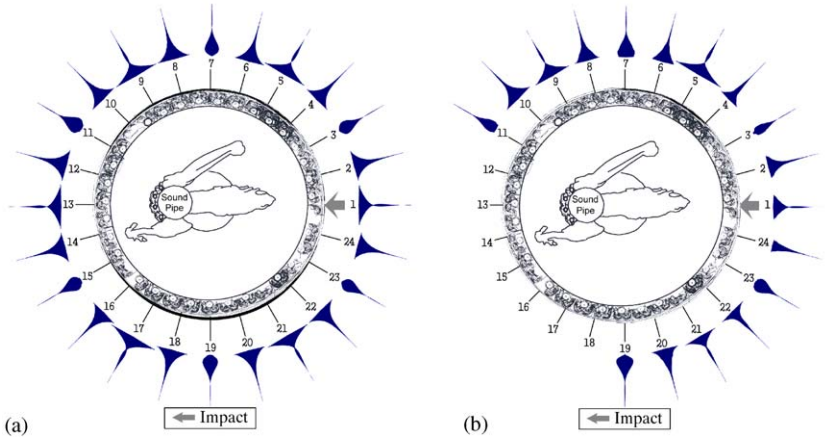

Fig. 13. Beat maps of the fundamental (*mode (0, 3)*): (a) vibration, (b) sound.

so on. It is ascertained again that wave patterns of the vibration and sound are repeated with the same periods along the circumference. This property indicates that the vibration beat maps can estimate the directivity of the sound beat. Comparing Figs. 11 and 13, the positions generating the clean beats are quite different from each other depending on the modes that produce the beat. In the next section, this phenomenon is investigated in detail using a mathematical model.

6. Analytical method for the beat maps

6.1. Beat model of the cylindrical shell

6.1.1. Impulse response of a slightly asymmetric shell

Based upon the modal expansion approach, the forced response of a shell structure can be expressed as

$$u_i(x,\theta,t) = \sum_{k=1}^{\infty} \eta_k(t) U_{ik}(x,\theta) \quad (i = 1,2,3). \tag{2}$$

In the mode function, U_{ik} $(i = 1, 2, 3)$ represent the principal components of the kth mode in the direction of x, θ, r in Fig. 14. The modal participation factor $\eta_k(t)$ of the kth mode is obtained with the condition that Eq. (2) should satisfy Love's equation of motion and mode functions should satisfy the eigenvalue problems [22].

By the orthogonality of the natural modes U_{ik}, the modal participation factor $\eta_k(t)$ satisfies the following uncoupled equation:

$$\ddot{\eta}_k + 2\varsigma_k \omega_k \dot{\eta}_k + \omega_k^2 \eta_k = F_k(t), \tag{3}$$

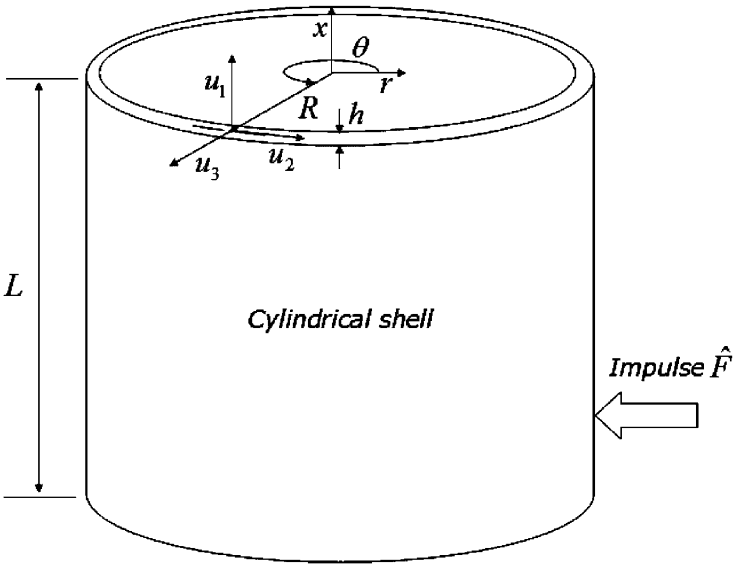

Fig. 14. Cylindrical shell under point impulse.

where

$$F_k(t) = \frac{\int_0^L \int_0^{2\pi} q_3 U_{3k} R \, \mathrm{d}x \, \mathrm{d}\theta}{\rho h N_k}, \tag{4}$$

$$N_k = \int_0^L \int_0^{2\pi} U_{3k}^2 R \, \mathrm{d}x \, \mathrm{d}\theta, \tag{5}$$

and where only the transverse force term q_3 is considered to describe the striking condition of the bell (i.e. $q_1 = q_2 = 0$). The condition of $|U_{3k}| \gg |U_{1k}|, |U_{2k}|$ is also applied since the transverse motion-oriented modes dominate the sound radiation. A modal damping factor ς_k is introduced to decouple the equation. ρ and h are used for the mass density and the thickness of the shell, respectively, while L is the length of the shell and R represents the radius of the shell.

By the Donnel–Mushtari–Vlasov's shell theory, the following orthogonal mode pair of the radial motion can be used to obtain the vibration response of the cylindrical shell [23]:

$$U_{3mn\gamma} = X_{3mn}(x) \cos n(\theta - \phi_\gamma) \quad (\gamma = L, H), \tag{6}$$

$$\phi_L = \theta_p, \quad \phi_H = \theta_p + \pi/2n. \tag{7,8}$$

In the case of an axi-symmetric shell, natural frequencies of this mode pair are the same regardless of the phase values. However, even with a small degree of asymmetry for a shell, they are not the same anymore. Hereafter, $(m, n)_L$ and $(m, n)_H$ are used for the mode pair of Eq. (6) while ω_{mnL}, ω_{mnH} represent their frequencies. ω_{mnL} represents a slightly lower frequency value than the frequency value of ω_{mnH}. In relation to the slight asymmetric effect, the modal characteristics have

been investigated on a ring with mass and stiffness asymmetry by Allaei and Soedel [24], on a ring with a cut by Hong and Lee [25], and on a cylindrical shell with a concentrated mass by Kim and Soedel [14]. Validity of the mode function given by Eq. (6) will be verified for the King Seongdeok Divine Bell with the measured mode data.

Using the mode pairs in Eq. (6), the response of the shell in Eq. (2) can be expressed as

$$u_3(x,\theta,t)=\sum_m\sum_n\sum_\gamma \eta_{mn\gamma}(t)U_{3mn\gamma}(x,\theta). \tag{9}$$

To determine a model for the impulse response, a point impulse shown in Fig. 14 is considered for Eq. (3). In this case, the force per unit area can be described as

$$q_3=\frac{\hat{F}}{R}\delta(x-x^*)\delta(\theta-\theta^*)\delta(t), \tag{10}$$

where $\hat{F}$ is the magnitude of the impulse, δ represents the Dirac delta function, and the point of impact is at (x^*,θ^*). Substituting Eq. (10) into Eq. (3) and applying the Laplace transform with zero initial conditions, the modal participation factor of each mode can be determined as

$$\eta_{mn\gamma}(t)=\frac{\hat{F}X_{3mn}(x^*)\ \cos n(\theta^*-\phi_\gamma)}{\omega_{mn\gamma}\rho hN_{mn}}\ \mathrm{e}^{-\varsigma_{mn\gamma}\omega_{mn\gamma}t}\sin(\omega_{mn\gamma}t), \tag{11}$$

where

$$N_{mn}=\pi R\int_0^L X_{3mn}^2(x)\,\mathrm{d}x. \tag{12}$$

Finally, from Eqs. (9) and (11), the impulse response of the cylindrical shell can be expressed as

$$\begin{aligned}u_3(x,\theta,t)=&\sum_m\sum_n\sum_\gamma\frac{\hat{F}X_{3mn}(x^*)X_{3mn}(x)\cos n(\theta^*-\phi_\gamma)\cos n(\theta-\phi_\gamma)}{\omega_{mn\gamma}\rho hN_{mn}}\\&\times\mathrm{e}^{-\varsigma_{mn\gamma}\omega_{mn\gamma}t}\sin(\omega_{mn\gamma}t).\end{aligned} \tag{13}$$

If the modal damping factor ($\varsigma_{mn\gamma}$) is very small, the velocity and the acceleration responses can be obtained as

$$\begin{aligned}\dot{u}_3(x,\theta,t)=&\sum_m\sum_n\sum_\gamma\frac{\hat{F}X_{3mn}(x^*)X_{3mn}(x)\cos n(\theta^*-\phi_\gamma)\cos n(\theta-\phi_\gamma)}{\rho hN_{mn}}\\&\times\mathrm{e}^{-\varsigma_{mn\gamma}\omega_{mn\gamma}t}\cos(\omega_{mn\gamma}t),\end{aligned} \tag{14}$$

$$\begin{aligned}\ddot{u}_3(x,\theta,t)=&-\sum_m\sum_n\sum_\gamma\frac{\omega_{mn\gamma}\hat{F}X_{3mn}(x^*)X_{3mn}(x)\cos n(\theta^*-\phi_\gamma)\cos n(\theta-\phi_\gamma)}{\rho hN_{mn}}\\&\times e^{-\varsigma_{mn\gamma}\omega_{mn\gamma}t}\sin(\omega_{mn\gamma}t).\end{aligned} \tag{15}$$

6.1.2. Beat of each mode

By extracting the particular mode terms from Eq. (15), the beat response of each mode can be obtained as

$$\ddot{u}_{3mn}(x,\theta,t) = -\frac{\omega_{mna}\hat{F}X_{3mn}(x^*)X_{3mn}(x)}{\rho h N_{mn}}\, e^{-\varsigma_{mna}\omega_{mna}t}[\cos n(\theta^* - \phi_L)\cos n(\theta - \phi_L)\sin(\omega_{mnL}t) + \cos n(\theta^* - \phi_H)\cos n(\theta - \phi_H)\sin(\omega_{mnH}t)] \quad (16)$$

where the average values of frequency and damping are used since these values for each pair are almost the same:

$$\omega_{mna} = (\omega_{mnL} + \omega_{mnH})/2 \quad \text{and} \quad \varsigma_{mna} = (\varsigma_{mnL} + \varsigma_{mnH})/2. \quad (17,18)$$

If the measurement position on the x-axis is located at $x = x^*$, the acceleration response on the circumference is determined as

$$\ddot{u}_{3mn}(x^*,\theta,t) = -C_{mn}e^{-\varsigma_{mna}\omega_{mna}t}[\cos n(\theta^* - \phi_L)\cos n(\theta - \phi_L)\sin(\omega_{mnL}t) + \cos n(\theta^* - \phi_H)\cos n(\theta - \phi_H)\sin(\omega_{mnH}t)], \quad (19)$$

where

$$C_{mn} = \frac{\omega_{mna}\hat{F}X_{3mn}(x^*)^2}{\rho h N_{mn}}. \quad (20)$$

The value of $-C_{mn}$ can be given as 1 for simplicity, since it is a constant for each mode With Eq. (19), the occurrence of a beat is predicted if the frequency pairs, ω_{mnL} and ω_{mnH}, are very close to each other. Using Eq. (19) as the analytical model, vibration wave for each mode can be obtained and the vibration distribution along the circumference can also be obtained.

6.2. The beat map drawing method

6.2.1. Analytical beat maps

An analytical beat map can be obtained by radially arraying the vibration waves by Eq. (19) at each point on the circumference. To determine the circumferential mode functions in Eq. (6), the method of least squares are applied to the measured modes.

Mode function $X_{3mn}(x)$ does not need to be determined precisely, because the modes of the hum and the fundamental have monotonous shapes along the height as shown in Fig. 6 for most of the Korean bells. They do not have any phase changes on the contour along the vertical axis. Therefore, although this function is left unknown in the analysis, the beat along the vertical axis could be easily estimated. If the mode shapes on the circumference are approximated from the measured modes, the beat maps from the analytical model in Eq. (19) will be very close to those obtained by the experiment. In the next section, it will be verified that the approximate mode functions are very closely matched to the measured results of the King Seong-deok Divine Bell.

6.2.2. Determination of the modal parameters for beat maps

The phases ϕ_L, ϕ_H in Eq. (19) are the most important parameters for the beat maps. The striking position θ^*, measured point θ, and the phase values determine the relative magnitudes of

the frequency components ω_{mnL} and ω_{mnH}. They determine the clarity and magnitude of a beat at each measuring point. Using the measured acceleration data at 24 different points on the circumference of the bell, the phase angles of the mode pairs can be determined by the method of least squares. The sum of the squared errors between the measured data and mode functions can be established as [26]

$$\varepsilon_\gamma = \sum_{j=1}^{24} [p_j - A_\gamma \cos n(\theta_j - \phi_\gamma)]^2 \quad (n = 2, 3 \text{ and } \gamma = L, H), \tag{21}$$

where p_j is the measured acceleration and A_γ is the scale factor used for each mode. By minimizing the sum of the squared errors for each mode number n, the phase angle and scale factor can be determined as

$$\frac{\partial \varepsilon_\gamma}{\partial A_\gamma} = 0, \quad \frac{\partial \varepsilon_\gamma}{\partial \phi_\gamma} = 0 \quad (\gamma = L, H). \tag{22, 23}$$

By using Eqs. (22) and (23), the phase angle ϕ_γ can be calculated from the following equation:

$$\frac{\sum p_j \cos n(\theta_j - \phi_\gamma)}{\sum p_j \sin n(\theta_j - \phi_\gamma)} - \frac{\sum \cos^2 n(\theta_j - \phi_\gamma)}{\sum \sin n(\theta_j - \phi_\gamma) \cos n(\theta_j - \phi_\gamma)} = 0 \quad (n = 2, 3 \text{ and } \gamma = L, H). \tag{24}$$

The calculated phase values with MATLAB 5.0 [27] are shown in Table 3. Modal damping factors are obtained by the logarithmic decrement method [28]. For the damping factor of each mode, it is necessary to measure the vibration at each node of *mode* $(m, n)_L$ and $(m, n)_H$ individually. As a result, damping factors of the mode pair were measured as almost identical in both the hum and the fundamental. The modal parameters for the beat maps of the hum and the fundamental are listed in Table 3.

6.2.3. *Verification of the mode functions*

As stated before, the accuracy of a beat map depends on the degree of closeness of the mode function $\cos n(\theta - \phi_\gamma)$ compared to the real circumferential mode of the bell. Using the *Modal Assurance Criteria* (MAC) [29], the correlation between the measured mode and the mode

Table 3
Modal parameters of the King Seong-deok Divine Bell

Parameter	*Mode (0, 2)*	Mode *(0, 3)*
ϕ_L	0.642 rad	−0.267 rad
ϕ_H	−0.143 rad	0.276 rad
ω_{mnL}	402.56 rad/s	1058.84 rad/s
ω_{mnH}	404.76 rad/s	1059.53 rad/s
ς_{mnL}	0.00013	0.00029
ς_{mnH}	0.00013	0.00030

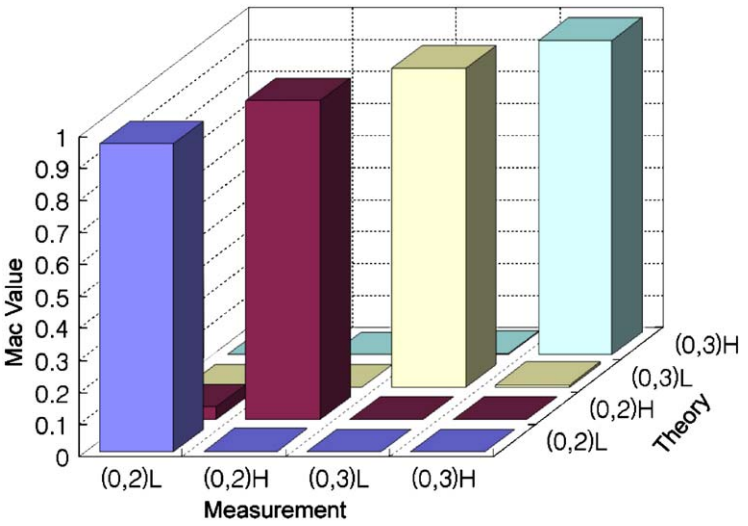

Fig. 15. MAC between the circumferential modes.

function can be estimated as

$$\mathrm{MAC}\left(\{p_E\}_i, \{p_A\}_j\right) = \frac{\left|\{p_E\}_i^{\mathrm{T}}\{p_A\}_j\right|^2}{\left(\{p_E\}_i^{\mathrm{T}}\{p_E\}_i\right)\left(\{p_A\}_j^{\mathrm{T}}\{p_A\}_j\right)}, \tag{25}$$

where $\{p_E\}_i$ is the measured mode vector and $\{p_A\}_j$is the analytical mode vector established by the mode function $\cos n(\theta - \phi_\gamma)$. Fig. 15 shows the calculated results of the MAC of the *mode* (*0, 2*) and the *mode* (*0, 3*). MAC exceeds 0.96 between the measured and analytical modes with the same n and γ, while it is less than 0.04 between different types of modes. This result assures that the measured modes of the King Seong-deok Divine Bell can be modeled by the harmonic functions and the calculated phase angles.

7. Beat maps by the analytical model

7.1. Beat map of the hum

Fig. 16 compares the beats of the hum at two different positions. The waves obtained by the analysis are almost identical to those by the measurement, except the initial short transient state. It means that phase angles and damping coefficients of the mode pair are appropriately determined. The vibration wave at Point 1 has a large amplitude, but the beat is not clear. On the contrary, the vibration wave at Point 3 is a clear beat with a relatively small magnitude. The reason for these phenomena is that, in Eq. (19), a response position as well as an excitation position influence the magnitudes of the frequency components ω_{02L} and ω_{02H}. As a result, at

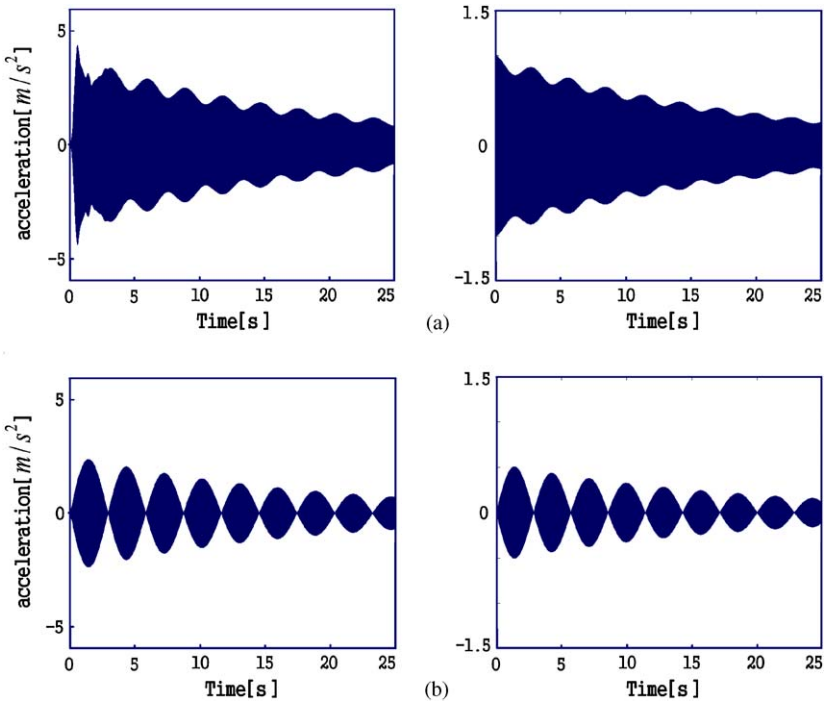

Fig. 16. Comparison of the beats in vibration of the hum (*mode (0, 2)*): (a) Point 1, (b) Point 3.

Point 3, *mode* $(0, 2)_L$ and *mode* $(0, 2)_H$ have almost identical amplitudes and a clear beat is generated.

The analytical beat map can be drawn by the same method as the one used in experimental beat map. When the analytical beat map in Fig. 17 is compared with the measured one in Fig. 11(a), both results are in good agreement for the beat distribution. Clear and unclear beats are repeated with the same interval along the circumference. As the mode pair has a periodic configuration along the circumference, the beat distribution also has this periodicity. As described above, the analytical beat map is available merely based on the measured mode data of the bell. It is interesting that vibration with large amplitude occurs periodically along the circumference. It will cause high stresses in some parts of the bell. This stress distribution is related to the life expectancy of the bell and may be another interesting research topic.

7.2. Beat map of the fundamental

The waves by an analytical model and from the measured data were confirmed to be same, except the initial short transient part. Fig. 18 displays an analytical beat map that is created by the same condition as in the experiment. The analytical beat map shows the same beat distribution characteristics as those of the experimental beat map in Fig 13 (a). Unlike the case of the hum, the striking at Dangjwa equally excites the mode pair $(0, 3)_L$ and $(0, 3)_H$. As a result, at all positions where the two modes respond equally, the amplitudes of the frequency components ω_{03L} and ω_{03H}

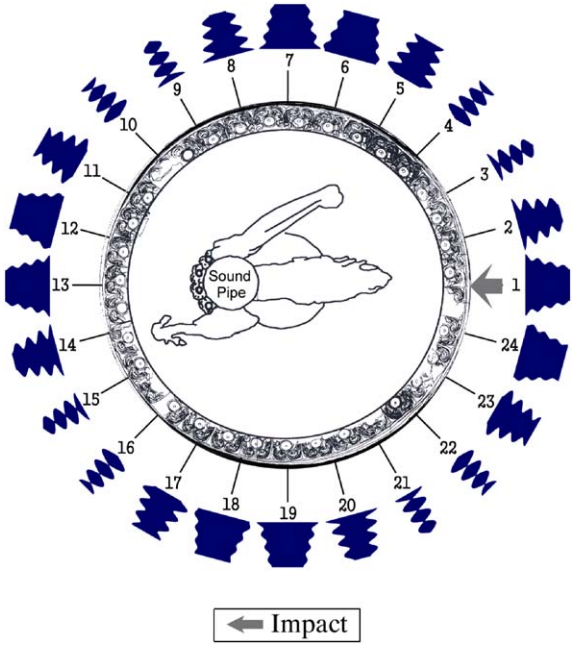

Fig. 17. Analytical beat map of the hum (*mode* (*0, 2*)).

in Eq. (19) are the same. With this condition, a clear beat with a large amplitude is generated at every $\pi/6$ radian incremental position from the striking point. Consequently, Dangjwa of the King Seong-deok Divine Bell seems to be at the optimal position on the circumference for the strong beat of the fundamental. In both the hum and the fundamental, the analytical beat maps can determine the positions where audiences can listen to the clear beat of each tone.

7.3. Considerations on the striking position

The striking point of the bell, called Dangjwa, is located at the center of percussion on the height of the bell. At the same time, Dangjwa on the circumference is desired to be on the position that produces the clear beat of the long-lasting hum. In this aspect, striking at Point 2 (30 cm right position from the center of the Dangjwa) of Fig. 6(a) is preferred, because it excites the mode pair of the hum equally. It is interesting to see how the beat map appears when striking at Point 2. The beat maps of the hum and the fundamental by the analytical method are shown in Fig. 19. In the hum, a clear beat with a large amplitude repeats by the period of $\pi/4$ from the striking point (Point 2), but the clear beat positions are different from those of Fig. 11. When the beat maps of Fig. 11(a) and Fig. 19(a) are compared, it is predicted that the striking at the Point 2, or other points satisfying the same excitation conditions, would produce a clearer and stronger beat for the long lasting hum. As seen from Fig. 18 and Fig. 19(a), a clear beat repeats with the period of $\pi/2n$ under the striking condition that excites *mode* $(m, n)_L$ and mode $(m, n)_H$ equally. However, a change of the striking position influences the beat characteristics of the important fundamental. The beat map in Fig. 19(b) displays how striking Point 2 may influence the beat of the

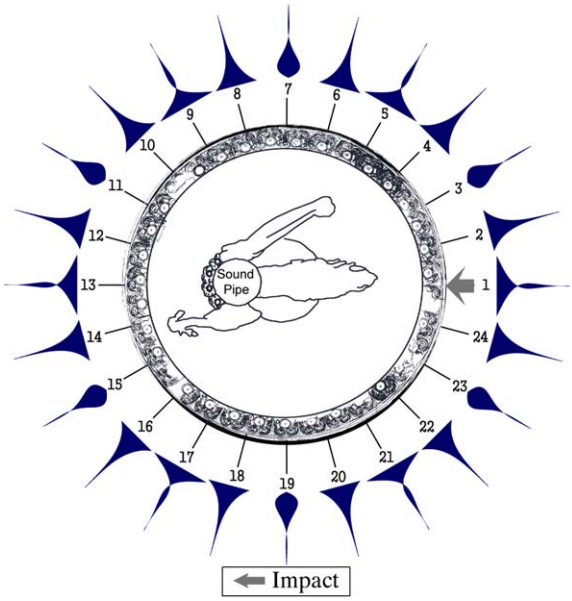

Fig. 18. Analytical beat map of the fundamental (*mode* (*0, 3*)).

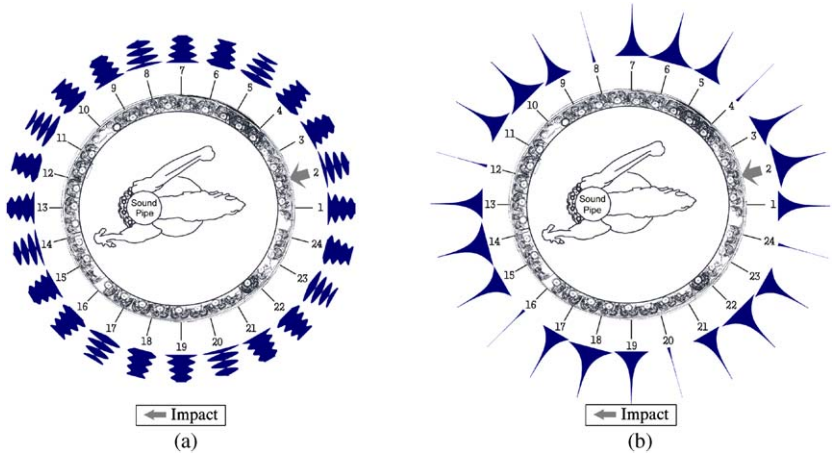

Fig. 19. Analytical beat maps under the striking at Point 2: (a) the hum, (b) the fundamental.

fundamental. As easily expected, because Point 2 is the node of the *mode* $(0, 3)_L$, the fundamental beat is not observed anywhere and several points (Points 4, 8, 12, 16, 20, and 24) do not produce the fundamental. As a result, if Point 2 is struck, the clearer beat of the hum will be produced while the fundamental will decay very monotonously. For the strong beats in both the hum and the fundamental, Points 5,11,17 and 23 will be the optimal striking positions because those positions can equally excite mode pairs in both *mode* (*0, 2*) and *mode* (*0, 3*). With these striking

positions, it is easily predicted that the beat maps of the two tones will be almost the same as shown in Figs. 19(a) and 18. Strong beats are generated in both the hum and the fundamental. However, it may be almost impossible to design the Dangjwa at these optimal striking positions because the slight asymmetric property occurring in the casting process is unpredictable. Consequently, the current Dangjwa of the King Seong-deok Divine Bell is located at the optimal position to produce a strong beat of the fundamental and a reasonable beat in the hum simultaneously.

8. Conclusion

The striking sound of the King Seong-deok Divine Bell has more than 50 frequency components below 1000 Hz and more than 130 components under 2000 Hz.These frequency components of the sound correspond to the natural frequencies of the bell body. Within several seconds after the striking, all partials except the 64 Hz hum and the 168 Hz fundamental disappear. 20 s after the striking, only the hum remains and it produces a long-lasting beating sound. As the important sound characteristics of the King Seong-deok Divine Bell, the beat in the hum has the period of 2.9 s and it makes the bell sound as if it were alive and breathing. The beat in the fundamental has the period of 9 s and it creates a clear and strong bell sound. The current striking position enables the beats to be produced in both the hum and the fundamental, and it especially generates a strong beat in the fundamental. To understand the beat distribution easily, the beat map for each partial tone was used. An analytical beat map drawing method was introduced, using the slightly asymmetric cylindrical shell model. The beat maps obtained by the analytical method were almost identical to those produced by the experiment. In the hum and the fundamental, it was found that the beat characteristics for clarity and strength repeated periodically on the circumference. The beat maps of the sound and the vibration showed the same periodical characteristics. When the mode pair is equally excited, the clear and unclear beats are repeated with the period of $\pi/2n$ on the circumference.

Acknowledgements

This study was continued under the Faculty Foreign Research Program in 2002 by Kangwon National University. The first author thanks Kangwon National University and University of the Pacific for providing an opportunity to become a visiting scholar. He also thanks Kyeongju National Museum in Korea that supported the experiment on the King Seong-deok Divine Bell.

References

[1] Y.H. Yum, A study on the Korean bells, Research Institute of Korean Spirits and Culture Report 84-14, 1984.
[2] T.D. Rossing, Acoustics of eastern and western bells, old and new, *Journal of the Acoustical Society of Japan* 10 (1989) 241–252.

[3] T.D. Rossing, A. Perrier, Modal analysis of a Korean bell, *Journal of the Acoustical Society of America* 94 (1993) 2431–2433.
[4] R. Perrin, T. Charnley, J. de Pont, Normal modes of the modern English church bell, *Journal of Sound and Vibration* 90 (1983) 24–49.
[5] R. Perrin, T. Charnley, A comparative study of the normal modes of various modern bells, *Journal of Sound and Vibration* 117 (1987) 411–420.
[6] R. Perrin, T. Charnley, G.M. Swallowe, On the tuning of church and carillon bells, *Applied Acoustics* 46 (1995) 83–101.
[7] B.H. Lee, A rating method for sound quality of braman bells, *Journal of the Acoustical Society of Korea* 1 (1982) 6–18.
[8] R. Perrin, A group theoretical approach to warble in ornamented bells, *Journal of Sound and Vibration* 52 (1977) 307–313.
[9] T.D. Rossing, Vibration of bells, *Applied Acoustics* 20 (1987) 41–70.
[10] S.H. Cheon, J.M. Lee, S.H. Kim, Y.H. Yum, A study on the vibration property of Korean bell, *Journal of the Korean Society for Mechanical Engineers* 13 (1989) 397–403.
[11] T. Charnley, R. Perrin, Studies with an eccentric bell, *Journal of Sound and Vibration* 58 (1978) 517–525.
[12] Kyungjoo National Museum, Comprehensive Research Reports on the King Songdok Divine Bell, 1999.
[13] R. Perrin, T. Charnley, H. Bandu, Increasing the lifetime of warble-suppressed bells, *Journal of Sound and Vibration* 80 (1982) 298–303.
[14] S.H. Kim, W. Soedel, J.M. Lee, Analysis of the beating response of bell typed structures, *Journal of Sound and Vibration* 173 (1994) 517–536.
[15] J.M. Lee, S.H. Kim, S.J. Lee, J.D. Jeong, H.G. Choi, A study on the vibration and sound characteristics of a lare size Korean bell, *Journal of Sound and Vibration* 257 (2002) 779–790.
[16] S.H. Kim, J.H. Kim, J.D. Jung, J.M. Lee, A study on the vibration and sound characteristics of the King Seong-deok Divine Bell, *Journal of the Korean Society for Noise and Vibration Engineers* 12 (2002) 534–541.
[17] Y.H. Yum, J.G. Gwak, J.H. Yoon, A study on the sound pipe of Korean bell, *Braman Bell* 5 (1982) 7–20.
[18] D.B. Yoon, Y.H. Kim, Experimenal analysis on acoustic characteristics of the sound pipe of King Seong-deok Bell, *Journal of the Acoustical Society of Korea* 16 (1997) 19–24.
[19] Y.H. Kim, S.H. Park, S.M. Kim, The effect of internal sound field and resonator on radiating sound of King Seong-deok Bell: proposing effective size of resonator, *Journal of the Acoustical Society of Korea* 16 (1997) 60–67.
[20] J.M. Lee, S.H. Kim, Correlation between design and characteristics of vibration and sound in King Seong-deok Devine Bell, *Collection of Papers on King Seong-deok Divine Bell* 1 (1999) 320–339.
[21] O. Dossing, Structural stroboscopy measurement of operational deflection shapes, *Sound and Vibration*, August (1988) 18–26.
[22] A.W. Leisa, *Vibration of Shells* NASA SP-288, US Government Printing Office, Washington D.C., 1973.
[23] W. Soedel, *Vibrations of Shells and Plates*, Marcel Dekker, New York, 1993.
[24] D. Allaei, W. Soedel, T.Y. Yang, Natural frequencies and modes of rings that deviate from perfect axisymmetry, *Journal of Sound and Vibration* 111 (1986) 9–27.
[25] J.S. Hong, J.M. Lee, Vibration of circular rings with local deviation, *Journal of Applied Mechanics* 61 (1994) 317–322.
[26] J.H. Mathews, *Numerical Method for Computer Science, Engineering and Mathematics*, second ed., Prentice-Hall, Englewood Cliffs, NJ, 1992.
[27] W. Palm, *Matlab for Engineering Applications*, McGraw-Hill, New York, 1999.
[28] L. Meirovitch, *Fundamentals of Vibrations*, McGraw-Hill, New York, 2001.
[29] N.M.M. Maia, J.M.M. Silva, *Theoretical and Experimental Modal Analysis*, Research Studies Press, Baldock, UK, 1997.